

Hydrogen Incorporation in Diamond: The Nitrogen-Vacancy-Hydrogen Complex

Claire Glover and M. E. Newton

Department of Physics, University of Warwick, Coventry CV4 7AL, United Kingdom

P. Martineau

DTC Research Centre, Belmont Road, Maidenhead, Berkshire SL6 6JW, United Kingdom

D. J. Twitchen

Element Six Ltd., King's Ride Park, Ascot, Berkshire SL5 8BP, United Kingdom

J. M. Baker

Clarendon Laboratory, University of Oxford, Parks Road, Oxford OX1 3PU, United Kingdom

(Received 3 December 2002; published 9 May 2003)

We report the identification of the nitrogen-vacancy-hydrogen complex in a freestanding nitrogen-doped isotopically engineered single crystal diamond synthesized by chemical vapor deposition. The hydrogen atom is located in the vacancy of a nearest-neighbor nitrogen-vacancy defect and appears to be bonded to the nitrogen atom maintaining the trigonal symmetry of the center. The defect is observed by electron paramagnetic resonance in the negative charge state in samples containing a suitable electron donor (e.g., substitutional nitrogen N_S^0).

DOI: 10.1103/PhysRevLett.90.185507

PACS numbers: 61.72.Ji, 81.05.Uw, 85.40.Ry, 76.30.Mi

Interest in a diamond grown by chemical vapor deposition (CVD) has been invigorated by recently reported advances in homoepitaxial synthesis of a single crystal diamond [1]. In this new material, electron and hole mobilities of 4500 and 3800 $\text{cm}^2 \text{V}^{-1} \text{s}^{-1}$, respectively, have been measured at room temperature. These values are approximately double the highest previously reported values [1]. In general, epitaxy on foreign substrates leads to a polycrystalline diamond, and the electronic and optical properties of grain boundaries preclude its use in some of the desired applications. A single crystal diamond with the reported carrier transport properties [1] could surpass other wideband gap materials for power and high frequency electronic applications [2]. Ultimately, the electrical and optical properties will be limited by defects and impurities grown into the material and introduced during the various diffusion, ion-implant, annealing, etc., processing steps involved in modern device fabrication, as well as possible degradation processes during device operation. This motivates work on understanding and determining the electronic properties and lattice structures of defects/impurities in a single crystal CVD diamond. In this Letter, we report the observation and identification of the nitrogen-vacancy-hydrogen complex in as-grown CVD diamond. We believe that this is the first point defect incorporating hydrogen in bulk diamond for which an atomic model (and hence the mode of hydrogen incorporation) has been determined. This defect is commonly found in CVD diamond (but not in a natural or high-temperature/pressure synthetic diamond), and, although its concentration is below our detection limits in the device grade material [1], it could still be present at very low levels trapping and/or scattering carriers.

Nitrogen is readily incorporated in CVD diamond in the form of a substitutional impurity (N_S) [3] and in the nearest nitrogen-vacancy complex [4]. The former is commonly observed in as-grown natural and high-temperature/pressure synthetic diamonds and the latter, although often present in unprocessed diamond, can be produced in high concentrations by radiation damage and annealing ($> 600^\circ\text{C}$), when mobile vacancies are trapped by N_S centers [5]. The neutral N_S center (N_S^0) is a very deep donor ($E_A = 1.7 \text{ eV}$) and has been extensively studied by electron paramagnetic resonance (EPR) and optical spectroscopic techniques [3]. It is not clear whether the nitrogen-vacancy center observed in CVD diamond is grown in as a unit or produced by N_S capturing a lattice vacancy that will be mobile at typical growth temperatures (e.g., $> 700^\circ\text{C}$). The nitrogen-vacancy center is an electron trap, capturing an electron from N_S^0 (producing N_S^+) and is often seen in both the negatively charged (NV^-) and the neutral (NV^0) charge state in the same sample. This serves as a warning: Diamond has a wide band gap (5.5 eV) and in many cases should be considered as an insulator; the concept of a Fermi level should be applied with caution [6].

Infrared absorption and EPR studies have provided information on hydrogen incorporation in polycrystalline CVD diamond films. Differently prepared polycrystalline films exhibit considerable differences in the shape of the C-H stretch absorption band (between 2700–3100 cm^{-1}), and the observed vibrational frequencies coincide with those measured in amorphous hydrogenated carbon (*a*-C:H), suggesting that the C-H stretch absorption originates from *a*-C:H incorporated in the film [7]. EPR studies on the H1 defect in polycrystalline diamond films

indicate that this defect, incorporating a hydrogen atom, is located on grain boundaries or in intergranular material rather than in the bulk diamond and that this defect accounts for only a small fraction of the total hydrogen [8–10]. In single crystal CVD diamond films, absorption bands have been attributed to incorporated hydrogen by comparing spectra in samples grown from carbon containing source gases and hydrogen and/or deuterium [11]. No models have been proposed for these complexes.

Hydrogen can compensate the substitutional boron acceptor ($E_A = 0.37$ eV) in diamond and the diffusion of hydrogen (deuterium) has been studied in *p*-type boron-doped diamond [12], although the site of the compensating hydrogen is unknown. We show here for the first time that the interaction of hydrogen with nitrogen should also be considered.

The freestanding single crystal diamond samples studied in this work were grown by microwave plasma CVD [1]. In the samples intentionally doped with nitrogen, N_S^0 ($< 2 \times 10^{18}$ cm $^{-3}$), NV^- ($< 2 \times 10^{16}$ cm $^{-3}$), and the new defect described in this Letter were detected by EPR. In undoped samples the N_S^0 concentration was below our detection limit, estimated to be 10^{15} cm $^{-3}$, and no other paramagnetic defects were detected. One of the samples was doped with ^{15}N (90% enrichment) to facilitate the EPR investigations described in this Letter. EPR measurements were made using a standard commercial spectrometer operating at approximately 9.6 GHz and at temperatures between 4.2 and 300 K. Infrared optical absorption measurements to determine the concentration of N_S^+ were made at room temperature [13].

An EPR spectrum observed in the ^{15}N doped sample is amenable to analysis and will be considered first. When the Zeeman field is oriented along a $\langle 100 \rangle$ cube axis, two high and low field satellite lines are observed, centered on a central system of four lines, as shown in Fig. 1. The

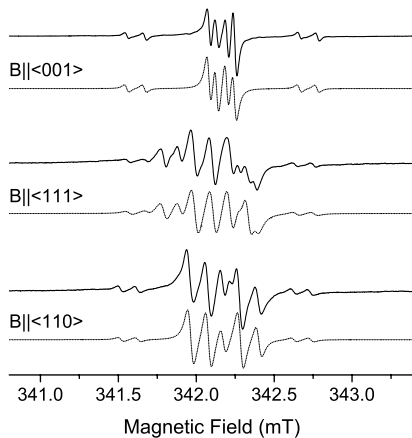


FIG. 1. EPR spectra observed in the ^{15}N doped sample. The experimental spectra (upper curves) were recorded at room temperature, with the magnet field oriented along $\langle 001 \rangle$, $\langle 111 \rangle$, and $\langle 110 \rangle$ directions. The simulations (lower curves) were obtained with the parameters given in the text.

separation between the mean position of the high and low field satellites is 1.04 mT, twice the nuclear Zeeman frequency of a proton in the average field of the two pairs of lines, indicating that these are *forbidden* electron-proton double spin flip transitions. The fact that each transition is split into two indicates an interaction with a second spin- $\frac{1}{2}$ nucleus. No successful reconstruction can be produced if this second nucleus is assumed to be another proton, and ^{13}C is ruled out since this isotope is only 1.1% abundant. ^{15}N , 90% abundant in this sample, is the obvious candidate. The central four lines are the *allowed* EPR transitions, split by the hyperfine interaction with two inequivalent $I = \frac{1}{2}$ nuclei. The spectrum is considerably more complicated when the Zeeman field is oriented along other directions (Fig. 1), but we find that the positions and relative intensities of all lines in the spectrum are fit by the following spin Hamiltonian:

$$H = \mu_B \underline{B} \cdot \underline{g} \cdot \underline{S} + \sum_j \underline{S} \cdot \underline{A}_j \cdot \underline{I}_j - \mu_N g_{Nj} \underline{B} \cdot \underline{I}_j, \quad (1)$$

where μ_B is the Bohr magneton, \underline{B} is the external magnetic field, \underline{g} is the electronic *g* matrix, \underline{A}_j is the hyperfine tensor which couples the electronic spin \underline{S} to the nuclear spin \underline{I}_j , μ_N is the nuclear magneton, and g_{Nj} the nuclear *g* factor associated with \underline{I}_j . The structure is accurately reproduced by assuming that this is a $S = \frac{1}{2}$ trigonal center (C_{3v} : threefold axis parallel to a $\langle 111 \rangle$ direction), with axially symmetric hyperfine interactions with one ^1H and one ^{15}N nucleus. The fit gives $g_{\parallel} = 2.0034(1)$, $g_{\perp} = 2.0030(1)$ [14], ^1H : $A_{\parallel} = 13.69(20)$ MHz and

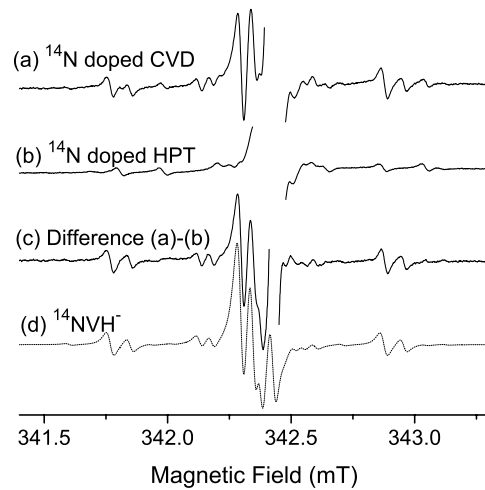


FIG. 2. (a) Room temperature EPR spectra ($B \parallel \langle 001 \rangle$) in ^{14}N doped single crystal diamond grown by CVD; the strong central transition from the $^{14}\text{N}_S^0$ center has been suppressed for clarity. (b) Room temperature EPR spectra in ^{14}N doped single crystal diamond grown at high temperature/pressure using the solvent/catalyst process. Only the $^{14}\text{N}_S^0$ center is observed, the central transition of which has been suppressed so that the ^{13}C hyperfine satellites are visible. (c) Removal of all transitions associated with $^{14}\text{N}_S^0$ in spectrum (a). (d) Simulation of $^{14}\text{NVH}^-$ using parameters described in the text.

$A_{\perp} = -9.05(20)$ MHz, and ^{15}N : $A_{\parallel} = \pm 2.94(10)$ MHz and $A_{\perp} = \pm 3.10(10)$ MHz, where in all cases “parallel” refers to the $\langle 111 \rangle$ symmetry axis of the defect. The signs of the ^1H hyperfine parameters have been chosen to be consistent with the interaction (predominately) originating from a dipole-dipole interaction. Further, if we assume that this interaction can be approximated as between separated electronic and nuclear dipoles, then the measured interaction gives an effective electron-proton separation of 2.2 Å. The small ^{15}N hyperfine coupling parameter indicates that less than 0.3% of the unpaired electron probability density is localized on the nitrogen atom.

Before we consider the identity of this defect, let us consider why it had not been identified in studies on ^{14}N doped single crystal CVD diamond. In many such studies there is a system of EPR transitions within ± 1 mT of the central EPR transition of the N_S^0 center [e.g., Fig. 2(a)]. These lines are not observed in a diamond grown at high pressures and temperatures and doped with a similar concentration of nitrogen [Fig. 2(b)]. As can be seen in Fig. 2, the central $^{14}\text{N}_S^0$ EPR transition ($|-\frac{1}{2}, 0\rangle \rightarrow |+\frac{1}{2}, 0\rangle$) and the associated natural abundance ^{13}C hyperfine satellites overlap the additional system of lines in the CVD sample, complicating analysis so much (especially in low symmetry directions) that little progress was made in identifying the defect. Second, for centers in which the ^{14}N hyperfine interaction is smaller than the quadrupole interaction, mixing of the spin states invalidates the EPR selection rule $\Delta M_S = 1$, $\Delta m_I = 0$, and the forbidden transitions become so strong that the hyperfine structure appears very complicated and hence difficult to recognize. We made the assumption that the defects observed in the ^{15}N and ^{14}N samples were structurally identical, took the predetermined g matrix and ^1H hyperfine parameters, and switched ^{14}N for ^{15}N (calculating the appropriate ^{14}N hyperfine parameters from the ^{15}N parameters). We also assumed that the quadrupole interaction was axially symmetric, included this interaction [15] in Eq. (1) and simulated the EPR spectra while allowing only the magnitude of this interaction to vary. Immediately, as shown in Fig. 2, we discovered that the defects were, as assumed, identical. The large ^{14}N quadrupole interaction [$P_{\parallel} = -4.8(1)$ MHz] together with the overlap from the $^{14}\text{N}_S^0$ EPR spectrum had concealed the truth about the nature of this center in the ^{14}N doped samples.

Let us now consider the identity of the new center. The EPR data shows that this defect incorporates a single proton and a single nitrogen atom, and in order to preserve the C_{3v} symmetry these two atoms must lie on the $\langle 111 \rangle$ symmetry axis of the defect. $\text{N}_S^{0/+}$ is present in relatively high concentration in the samples in which we observe the new center, so we should consider this defect as a potential trap for hydrogen. To first order, the properties of N_S^0 are explained as follows: the nitrogen atom forms three equivalent bonds with carbon neighbors; in the direction of the fourth neighbor we find a lone pair

of electrons on the nitrogen and an unpaired electron predominately localized in the orbital on the unique carbon neighbor (C_a) pointing toward the nitrogen [3]. Both C_a and the nitrogen relax back so that this bond is about 25% longer than the normal C-C bond [3]. Hydrogen could be incorporated into this extended bond, bonding to the carbon ($\text{C}_a\text{—H:N}_S$) 0 , but this defect would be diamagnetic and thus could not be the new center reported here. The positively charged complex ($\text{C}_a\text{—H}\cdot\text{N}_S$) $^+$ or ($\text{C}_a\cdot\text{H—N}_S$) $^+$ would have $S = \frac{1}{2}$ and the correct symmetry; however, the hydrogen and nitrogen hyperfine interactions would be far larger than observed, and we could not explain the charge state. Hence, we rule out the *bond-centered hydrogen-substitutional nitrogen complex*. The unpaired electron probability density on the proton and the nitrogen atom is very small and, in the latter case, is similar to that measured for the NV^- center [16,17]. For the NV^- center $> 70\%$ of the unpaired electron probability density is localized on the three carbon dangling orbitals [18]. We know that nitrogen-vacancy centers are grown into CVD diamond, so we are led to consider the properties of the complex formed by trapping a hydrogen atom in the vacancy of a nitrogen-vacancy center (the NVH complex). If the hydrogen atom were bonded to the nitrogen, we would have a defect with C_{3v} symmetry, as required. For $S = \frac{1}{2}$ we need an odd number of electrons localized in the three dangling carbon orbitals; this would mean that the NVH complex detected by EPR must be either NVH^- or NVH^+ . We know that it is the former because, in the samples studied, infrared and EPR measurements show that $[\text{N}_S^+] \approx [\text{NVH}^-]$ [19], indicating the charge transfer reaction $\text{N}_S^0 + \text{NVH}^0 \rightarrow \text{N}_S^+ + \text{NVH}^-$. NVH^- would have five electrons in the a_1 and e levels derived from the carbon dangling orbitals [4], and the ground state would be 2E , which is consistent with the measured EPR parameters. No static Jahn-Teller splitting of the 2E ground state is observed, suggesting that any such distortion is dynamic, as is the case for the ground state of the neutral vacancy in diamond [20]. No “freezing in” of a lower symmetry was observed while studying the center down to 4.2 K.

The NVH^- model is consistent with all the measured EPR properties of the defect. Since the unpaired electron is localized in the carbon dangling orbitals, we would expect an axially symmetric g matrix with a small anisotropy, consistent with what is observed. The proton hyperfine interaction suggests an electron-proton separation of 2.2 Å. If we take the N-H bond length to be 1.04 Å, then in an undistorted T_d nitrogen vacancy the distance between one of the three equivalent carbon atoms of the vacancy and the hydrogen would be 1.8 Å. However, a significant outward relaxation of the nearest neighbors is expected (e.g., 0.15–0.25 Å for the vacancy in diamond) [21], and a mean outward relaxation of $\approx 15\%$ of the normal C-C bond length would give a nearest-neighbor carbon to proton separation of 2.2 Å. The small nitrogen hyperfine interaction is consistent with the NVH^- model,

since the unpaired electron probability density is localized on the three carbon dangling orbitals that have little overlap with the nitrogen or hydrogen. ^{13}C hyperfine satellites of the correct intensity for three equivalent carbon neighbors have been observed, and preliminary analysis suggests that the majority of the unpaired electron probability density is to be found on these atoms. The large quadrupole interaction, similar in magnitude to that in the NV^- center [16,17], is consistent with the NVH^- model and with previous calculations [22].

Since the NVH^- center is observed in as-grown material, we know that it is stable to $\approx 900^\circ\text{C}$. The stability is such that configurations involving a weak nitrogen-hydrogen bond (e.g., H in the backbonding position) can be ruled out (furthermore, such a position would not be consistent with the measured EPR parameters). Hydrogen diffusion has been observed only in *p*-type diamond [12], when the rapidly diffusing species is H^+ . This charge state is not expected in the nitrogen doped samples, so it appears unlikely that the NVH^- center is formed by $\text{H}^{0/-}$ diffusing to a $\text{NV}^{-/0}$ center in the bulk diamond. It appears more likely that surface N-H is overgrown and that either the vacancy is grown in or diffuses to the center. Both mechanisms are under experimental and theoretical investigation.

In summary, the NVH^- center has been observed in as-grown CVD diamond, the hydrogen atom is apparently bonded to the nitrogen, and the unpaired electron probability density is located in the dangling orbitals of the three equivalent nearest-neighbor carbon atoms, with very little localization on the nitrogen. NVH^- is commonly found in single crystal and polycrystalline diamond samples grown in different laboratories, where the nitrogen contamination is often accidental. In polycrystalline samples the complexity of the NVH^- EPR powder pattern spectrum means that its EPR spectrum is often obscured by other defects (e.g., N_5^0 , H1, etc.). NVH^- has been shown to be an electron trap; the stability and electronic properties of this defect are under investigation. The identification of this center was facilitated via isotopic substitution and EPR spectroscopy. It is clear that this approach shows great promise for providing a complete description of defects and impurities in single crystal CVD diamond, an important new semiconducting material. The discovery of NVH^- could impact on the use of the NV^- center in quantum cryptography [23], as the latter could be transformed to the former by trapping hydrogen.

We acknowledge the invaluable help with sample preparation/characterization provided by Samantha Quinn, Andy Taylor, Chris Kelly, and Jacques Jones of the DTC Research Centre.

- [1] J. Isberg, J. Hammersberg, E. Johansson, T. Wikstrom, D.J. Twitchen, A.J. Whitehead, S.E. Coe, and G.A. Scarsbrook, *Science* **297**, 1670–1672 (2002).
- [2] G.A.J. Amaratunga, *Science* **297**, 1657–1658 (2002).
- [3] M.E. Newton, in *Properties, Growth and Applications of Diamond*, edited by M.H. Nazare and A.J. Neves, Chap. A5.4, pp. 136–140.
- [4] J.P. Goss, R. Jones, P.R. Briddon, G. Davies, A.T. Collins, A. Mainwood, J.A. van Wyk, J.M. Baker, M.E. Newton, A.M. Stoneham, and S.C. Lawson, *Phys. Rev. B* **56**, 16031–16032 (1997).
- [5] Y. Mita, *Phys. Rev. B* **53**, 11360–11364 (1996).
- [6] A.T. Collins, *J. Phys. Condens. Matter* **14**, 3743–3750 (2002).
- [7] B. Dischler, C. Wild, W. Müller-Sebert, and P. Koidl, *Physica (Amsterdam)* **185B**, 217–221 (1993).
- [8] X. Zhou, G.D. Watkins, K.M. Rutledge, R.P. Messmer, and S. Chawla, *Phys. Rev. B* **54**, 7881–7890 (1996).
- [9] D.F. Talbot-Ponsonby, M.E. Newton, J.M. Baker, G.A. Scarsbrook, R.S. Sussmann, and A.J. Whitehead, *Phys. Rev. B* **57**, 2302 (1998).
- [10] D.F. Talbot-Ponsonby, M.E. Newton, J.M. Baker, G.A. Scarsbrook, R.S. Sussmann, A.J. Whitehead, and S. Pfenninger, *Phys. Rev. B* **57**, 2264 (1998).
- [11] F. Fuchs, C. Wild, K. Schwarz, W. Müller-Sebert, and P. Koidl, *Appl. Phys. Lett.* **66**, 177 (1995).
- [12] J. Chevallier, A. Lussou, D. Ballutaud, B. Theys, F. Jombard, A. Deneuve, M. Bernard, E. Gheeraert, and E. Bustarret, *Diam. Relat. Mater.* **10**, 399 (2001).
- [13] S.C. Lawson, D. Fisher, D.C. Hunt, and M.E. Newton, *J. Phys. Condens. Matter* **10**, 6171–6180 (1998).
- [14] We have taken the g value of the N_5^0 EPR center to be 2.0024 and used this as a reference for the determination of the g values.
- [15] The quadrupole interaction \mathbf{P} adds a term $\mathbf{I} \cdot \mathbf{P} \cdot \mathbf{I}$ to Eq. (1). See A. Abragam and B. Bleaney, *Electron Paramagnetic Resonance* (Dover, New York, 1986).
- [16] X.F. He, N.B. Manson, and P.T.H. Fisk, *Phys. Rev. B* **47**, 8816–8822 (1993).
- [17] Our unpublished ^{14}N parameters differ slightly: $A_{\parallel} = \pm 2.16(10)$ MHz, $A_{\perp} = \pm 2.61(10)$ MHz, and $P_{\parallel} = -5.05(10)$ MHz (\parallel refers to the defect $\langle 111 \rangle$ -symmetry axis).
- [18] J.H.N. Loubser and J.A. van Wyk, *Rep. Prog. Phys.* **41**, 1201–1248 (1978).
- [19] [X] represents the concentration of species X.
- [20] G. Davies, *Rep. Prog. Phys.* **44**, 787–830 (1981).
- [21] J.A. van Wyk, O.D. Tucker, M.E. Newton, J.M. Baker, G.S. Woods, and P. Spear, *Phys. Rev. B* **52**, 12657–12667 (1995).
- [22] J.M. Baker and M.E. Newton, *Appl. Magn. Reson.* **7**, 209–235 (1994).
- [23] A. Beveratos, R. Brouri, T. Gacoin, A. Villing, J.P. Poizat, and P. Granger, *Phys. Rev. Lett.* **89**, 187901–187904 (2003).